Available online at www.sciencedirect.com
SCIENCE DIRECT®
Carbohydrate Research 340 (2005) 2144–2149
Carbohydrate RESEARCH

Pectin–chitosan multilayer formation

Mariya Marudova,† Simone Lang, Geoffrey J. Brownsey and Stephen G. Ring*

Division of Food Materials Science, Institute of Food Research, Norwich Research Park, Colney, Norwich NR4 7UA, UK

Received 20 September 2004; accepted 7 July 2005
Available online 28 July 2005

Abstract—The deposition of alternating layers of pectin and chitosan at a solid surface was studied using surface plasmon resonance. The binding of biopolymer to the surface was irreversible over the time scales examined. The deposition was dependent on the flow rate through the measurement cell with mass transport limitation at lower flow rates. The thickness of the deposited layer was dependent on the biopolymer concentration and was particularly marked for pectin. This was consistent with a process of initial attachment, followed by a slower structural rearrangement, which was inhibited at high initial surface concentrations of adsorbed biopolymer. Sequential deposition resulted in the formation of multilayers with an essentially linear growth rate.

Keywords: Pectin; Chitosan; Multilayer; Surface plasmon resonance

1. Introduction

The attraction between oppositely charged polyelectrolytes can create a range of structures, including complexes,[1,2] coacervates,[3] networks and multilayers.[4] If a dilute solution of polyelectrolyte is titrated with a dilute solution of an oppositely charged polyelectrolyte[5] then initially it may be possible to form soluble polyelectrolyte complexes. As the charge ratio on the polyelectrolytes approaches unity, then an associative phase separation/precipitation is often observed. As further polyelectrolyte is added, then redissolution of the precipitate may occur as a result of charge reversal. The driving force for complex formation can include coulombic interactions, and an entropic contribution from the 'release' on complexation of low molecular weight counterions associated with the polyelectrolyte.[6] The complexation shows an ionic strength dependence as a result of screening effects and the dependence of the magnitude of the effect of counterion release on ionic strength. For systems containing weak polyelectrolytes, the interactions show a strong dependence on pH.

These attractive interactions have been used to fabricate multilayer structures using layer-by-layer assembly. These are generally regarded as non-equilibrium structures. A requirement for multilayer formation is that the addition of an oppositely charged polyelectrolyte to a charged surface results in charge reversal, normally depicted as loops and trains of the polyelectrolyte extending from the surface. Charge reversal permits successive deposition of oppositely charged polyelectrolytes. While many studies have been performed with synthetic polyelectrolytes, there are fewer reports on the formation of multilayers using biopolyelectrolytes. Recent examples include poly-L-lysine/alginate;[7] poly-L-lysine/hyaluronan;[8] and chitosan/hyaluronan.[9] For these weak polyelectrolytes, the structure of the multilayer is influenced by pH[8,10,11] and ionic strength.[12,13] A further variable is the extent to which the two polyelectrolytes interpenetrate,[14] and the extent of crosslinking and charge neutralisation of one polymer by another. For multilayer growth, both linear and exponential growth regimes have been found,[15,16] within the latter case the diffusion of one polyelectrolyte to the surface of the growing layer leading to an increasing

* Corresponding author. Tel.: +44 (0)1603 255000; fax: +44 (0)1603 507723; e-mail addresses: margo@pu.acad.bg; steve.ring@bbsrc.ac.uk;
† University of Plovdiv 'Paisii Hilendarski', 24 Tzar Assen, 4000 Plovdiv, Bulgaria.

0008-6215/$ - see front matter © 2005 Elsevier Ltd. All rights reserved.
doi:10.1016/j.carres.2005.07.004

layer thickness. At present the proposed applications of biopolyelectrolyte multilayers are largely in the biomedical area as encapsulation systems, and coatings which can control cell adhesion,[7,9,17] although their functionality is relevant to other sectors including food.

In this article, we wish to consider the interaction between two oppositely charged weak biopolyelectrolytes, pectin and chitosan. Pectic polysaccharides are components of the primary cell wall and middle lamella of dicotyledonous plants. They are structurally complex and heterogeneous polyelectrolytes,[18,19] consisting of linear regions of (1→4)-α-D-galacturonosyl units and their methyl esters, interrupted in places by (1→2)-α-L-rhamnopyranosyl units. A fraction of these rhamnopyranosyl residues are branch points for neutral sugar side chains of (1→5)-α-L-arabinofuranosyl or (1→4)-β-D-galactopyranosyl residues. The average spacing between charges along the galacturonosyl backbone is inversely related to the methyl ester content, furthermore the charge may be randomly distributed, or may occur in blocks of contiguous uronic acid residues. Studies on the conformation of pectin in dilute and moderately concentrated solution suggest an expanded conformation with a relatively high intrinsic viscosity.[20] Pectins can form network structures with divalent counterions such as Ca^{2+} and basic biopolyelectrolytes including chitosan[21] and poly-L-lysine.[22] Controlling charge and its distribution along the pectin chain is a potentially powerful approach to modifying the properties of pectin-containing structures.

Chitosan is obtained by the alkaline or enzyme N-deacetylation of chitin to produce (1→4)-β-D-glucosamine chains. Chitosan has an expanded conformation in dilute aqueous solution, which is dependent on the degree of acetylation of the chitosan and charge.[23,24] Both pectin and chitosan can be classified as semi-flexible polymers. In this article, we examine the interaction between chitosan and pectin using surface plasmon resonance.

2. Experimental

2.1. Materials

Citrus pectin with a degree of esterification of 36.6% was obtained from CP Kelco. Low molecular weight chitosan, with a reported degree of deacetylation of 75–85% was obtained from Sigma.

2.2. Surface plasmon resonance

A Biacore instrument was used with a Biacore sensing chip consisting of a glass slide coated with a thin (~50 nm) layer of gold. The SPR response causes a shift in the angle $\Delta\theta$ of the SPR minimum in reflected light intensity and is associated with changes in refractive index at the gold surface. For the Biacore instrument, a response of 10,000 resonance units is equivalent to a $\Delta\theta$ of 1°. The resonance response was calibrated at 20 °C using sucrose/water and methanol/water mixtures of known refractive index, up to a maximum refractive index of 1.3811. The response was linear in this region with a $\Delta\theta$ of 86.6° per change in refractive index of unity. The gold surface of the surface plasmon resonance chip was initially coated with poly-L-lysine, 0.08 mg/mL in 0.01 M NaOH 0.1 M NaCl, in the measurement cell.[25] Under these conditions, the observed binding of poly-L-lysine was irreversible, and the bound poly-L-lysine has a disordered conformation.[25] After multilayer build-up, the poly-L-lysine surface layer was regenerated by flowing 0.01 M NaOH through the measurement cell. The observed binding to the same poly-L-lysine base layer, over the course of several hours, showed good reproducibility (better than ±5%). The maximum observed variability with different chips and base layers was ±20%.

2.3. Photon correlation spectroscopy

The apparatus employed was an ALV/SP-86 spectrogoniometer (ALV, Langen, Germany) equipped with a Coherent Radiation Innova 100-10 vis Argon Ion laser operating at 0.5 W and wavelength of 514 nm. The scattered light intensity was monitored using an ALV/PM-15 ODSIII detection system at a fixed scattering angle of 90°. After amplification and discrimination, signals were directed to an ALV/5000E digital multiple-tau correlator and time-intensity correlation functions recorded, typically for 600 s duration. Size distribution functions were computed using the appropriate Windows-based ALV software, which incorporated regularised inverse Laplace transform and ALV-CONTIN packages. Additional analysis was undertaken using Origin V6 (Microcal) proprietary software. Pectin and chitosan were dissolved in 50 mM acetate buffer 100 mM NaCl at pH 5.6 and then directly filtered through a 0.22 μm filter into the cuvette. For a particle in solution subject to Brownian motion, the translational diffusion coefficient is related to the measured intensity correlation function $g^{(2)}\tau$ by the expression[26]

$$g^{(2)}\tau = 1 + \exp(-2D_t k_s^2 \tau) \quad (1)$$

where k_s, the scattering vector, is given by

$$k_s = \frac{4\pi n}{\lambda} \sin\frac{\theta}{2} \quad (2)$$

where n is the refractive index of the solution, θ, the scattering angle and λ the wavelength of light. For the diffusion of particles in dilute solution, the hydrodynamic radius of the particle, R_h, may be obtained from

$$D_t = kT/6\pi\eta R_h \quad (3)$$

where η is the solvent viscosity, and k and T have their usual meanings.

3. Results and discussion

The pectin was characterised in the previous research,[22] it had a galacturonic acid content of ~90% and a degree of esterification of ~36%. The distribution of charged residues was determined using a chemical fragmentation procedure[27] and was essentially random.[22] The pK_a of the glucosamine in chitosan is ~6.5 and is dependent on ionic strength and chitosan structure, more particularly the degree of acetylation.[28] The carboxylate of the galacturonic acid of pectin has a pK_a of ~3.5.[29] Previous research[21,22] has examined the gelation of chitosan and pectins differing in degree of esterification over the range 30–70%. It was found that pectin/chitosan mixtures formed network structures at pH 5.6 where both polymers carried a charge. At pH 5.6, the carboxyl group of pectin is essentially fully dissociated. At this pH, the degree of dissociation of the ammonium groups of the glucosamine residues of chitosan is ~0.2 for a chitosan of a low degree of acetylation.[28] In the present investigation with a reported degree of deacetylation of the chitosan of 85%, and a pectin which consists of 90% galacturonic acid of which 36% is methyl esterified, charge balance at pH 5.6 occurs at a pectin/chitosan ratio of ~1.2 to 1.

Poly-L-lysine can both crosslink pectin networks and under appropriate conditions, bind to a gold surface with a high affinity. Therefore, in order to study pectin and chitosan adsorption by surface plasmon resonance, the gold surface of a surface plasmon resonance chip was initially coated with poly-L-lysine to form a positively charged base layer. After the initial deposition of poly-L-lysine, the surface was rinsed with 50 mM acetate buffer containing 0.1 M NaCl at pH 5.6. Preliminary experiments examined the effect of sample flow rate on the kinetics of association of the biopolymer to the surface of the growing multilayer at this pH. In surface plasmon resonance experiments, the mass transport of molecules to the diffusion boundary layer can have an effect on the observed kinetics of binding. In Figure 1a is shown the effect of flow rate through the measurement cell on the binding of pectin (0.08 mg/mL) to the initial poly-L-lysine layer for flow rates in the range 0.017–0.83 μL s^{-1}. The resonance response was normalised relative to the limiting plateau of response at longer times. The observed behaviour showed a marked dependence on the flow rate at flow rates of 0.017 and 0.083 μL s^{-1} but became essentially independent of flow rate >0.42 μL s^{-1}. For the binding of chitosan to the pectin layer at pH 5.6 (Fig. 1b) a similar trend was observed although the effect at the lower flow rates was less marked. The Onsager coefficient of mass transport, L_m, is given by

$$L_m \approx \sqrt[3]{\frac{D^2 f}{h^2 w l}}$$

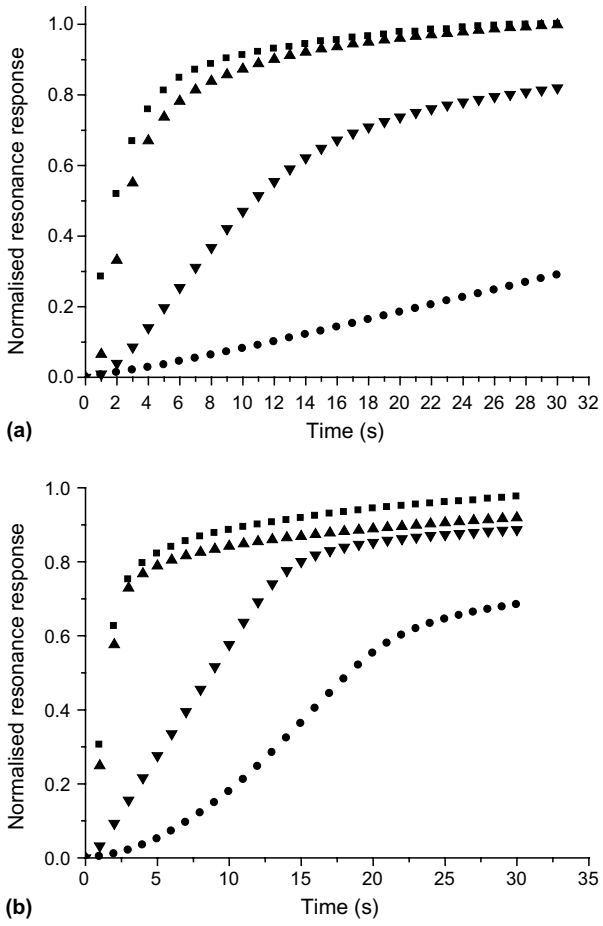

Figure 1. (a) A plot of normalised resonance response versus time for pectin deposition on a poly-L-lysine layer at flow rates of 0.83 (■); 0.42 (▲); 0.083 (▼) and 0.017 (●) μL s^{-1}. (b) A plot of normalised resonance response versus time for chitosan deposition to a pectin layer at pH 5.6 at flow rates of 0.83 (■); 0.42 (▲); 0.083 (▼) and 0.017 (●) μL s^{-1}.

where D is the coefficient of diffusion, f rate of flow, and h, w and l the dimensions of the flow cell which are 50, 500 and 2400 μm, respectively, with a total volume of 0.06 μL. Estimates of the diffusion coefficient, D_t, of chitosan and pectin were obtained by photon correlation spectroscopy. Light scattering studies on the solution behaviour of polysaccharides, including pectin and chitosan,[20,23,30–32] are inevitably complicated by the presence of aggregated material. In this study, larger aggregates were removed by filtration. The measured value of D_t for chitosan and pectin were 3.2×10^{-12} m^2 s^{-1} and 1.7×10^{-12} m^2 s^{-1}, respectively. The value obtained for pectin is similar to that obtained for a pectin fraction having a weight average molecular weight of 1×10^6 g mol^{-1}, with a D_t, of 1.2×10^{-12} m^2 s^{-1}. For a low molecular weight chitosan of M_w 44,000 the reported D_t at pH 4.5 was 1.98×10^{-11} m^2 s^{-1}. For chitosans with a low degree of acetylation, a pH dependent aggregation was observed at higher pH's with an onset in the region of pH 5.5–7.0.[33] The value obtained in the current study

is indicative of some aggregation, or higher molecular weight. For the adsorption of both pectin and chitosan, the change to mass transport limited behaviour occurs for calculated values of L_m of $<7 \times 10^{-7}$ m s^{-1}. The observed differences in the binding behaviour of chitosan and pectin are consistent with their measured values of D_t. An estimate of the thickness of the boundary layer, d, is given by[34,35]

$$d \approx \sqrt[3]{\frac{Dh^2wl}{f}}$$

For the flow rates used, the boundary layer thickness ranges from 1.5 to 8.3 μm.

The stability of a poly-L-lysine/pectin/chitosan multilayer formed at pH 5.6 from 0.08 mg/mL solutions of chitosan and pectin was examined as a function of pH over the pH range 3.6–8.0 at salt concentrations ranging from 0.05 to 0.15 M NaCl. Over the pH range 3.6–7, the layers were stable (>100 s). At an ionic strength of 0.15 M, changing the pH to 8 resulted in removal of the chitosan layer. Reducing the ionic strength to 0.05 M resulted in substantial removal of the pectin layer as well ~60%. As at pH 8.0, the charge on the chitosan is essentially fully suppressed, the stability of the chitosan/pectin interaction appears wholly dependent on the electrostatic interactions between chitosan and pectin.

The effect of biopolymer concentration, in the range 0.005–0.08 mg/mL, at a flow rate of 0.417 μL s^{-1} on the association at the surface at pH 5.6 as a function of time is shown in Figure 2a and b for pectin and chitosan, respectively. The binding is shown for the deposition of pectin on a poly-L-lysine/pectin/chitosan multilayer, and for the deposition of chitosan on a poly-L-lysine/pectin/chitosan/pectin multilayer. The binding to a layer which was formed at a flow rate of 0.42 μL s^{-1} and a concentration of 0.04 mg/mL was examined. For both biopolymers, the rate of association shows a concentration dependence. Plots of the initial rates of adsorption measured as $\Delta\theta$ s^{-1} versus concentration are linear with slopes of 64 and 56 deg s^{-1} per mole of anhydrohexose unit for chitosan and pectin, respectively. The density of the polysaccharides on the surface at saturation shows a concentration dependence, which is marked in the case of pectin and weaker for chitosan. The extent of adsorption of flexible polymers on a solid surface from solution is often influenced by polymer concentration. Polymer adsorption is frequently a non-equilibrium process and irreversible over practical timescales.[36] Following an initial contact and attachment to the surface, there is a process of structural rearrangement and spreading of the polymer on the surface.[37,38] For many biopolymers, this spreading process is slow as a result of their relatively rigid structure, which gives rise to slow structural rearrangement. If

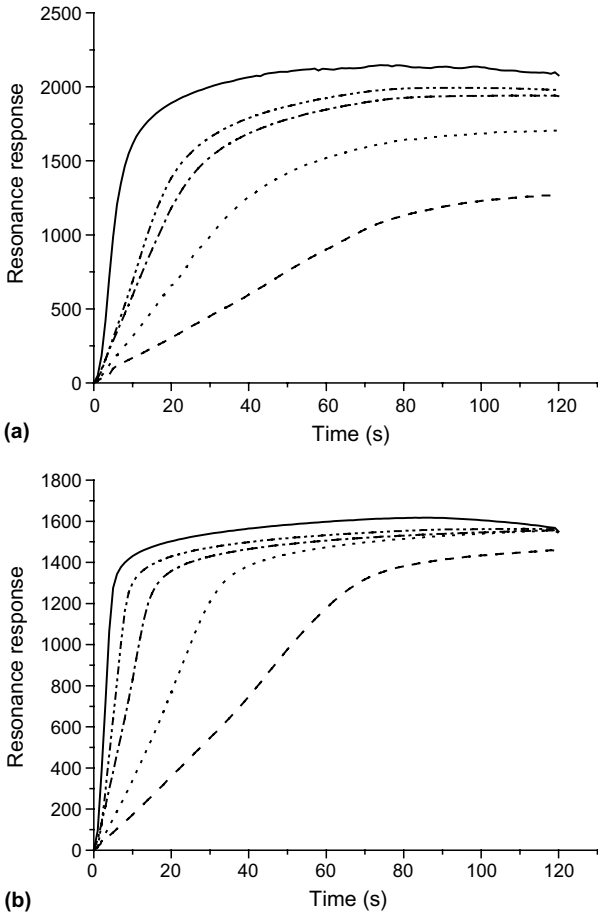

Figure 2. (a) Plot of resonance response versus time for the adsorption of pectin on a chitosan layer at a flow rate of 0.42 μL s^{-1}, at concentrations of pectin of 0.005 (---); 0.01 (· · ·); 0.02 (–·–·–); 0.04 (···–··) and 0.08 (—) mg/mL. (b) Plot of resonance response versus time for the adsorption of chitosan on a pectin layer at a flow rate of 0.42 μL s^{-1}, at concentrations of chitosan of 0.005 (---); 0.01 (· · ·); 0.02 (–·–·–); 0.04 (···–··) and 0.08 (—) mg/mL.

the rate of attachment of polymers at the surface is fast compared to the rate of structural rearrangement, the binding of polymers to the surface will impede the spreading process. As a result with increasing concentration, and the rate of attachment, the amount of polymer adsorbed at saturation increases. The observed binding behaviour of pectin and chitosan is consistent with this model, with the more marked concentration-dependent behaviour of pectin being attributed to its larger molecular size and consequently slower spreading rate.

A multilayer was fabricated by sequential deposition of pectin and chitosan both at 0.08 mg/mL in the acetate buffer at pH 5.6 at a flow rate of 25 μL/min for 2 min. Between each addition of biopolymer the sensor surface was rinsed with the acetate buffer for 2 min. Figure 3a shows the surface plasmon resonance response for the build up of a 18-layer multilayer, starting with a pectin layer followed by successive addition of low molecular

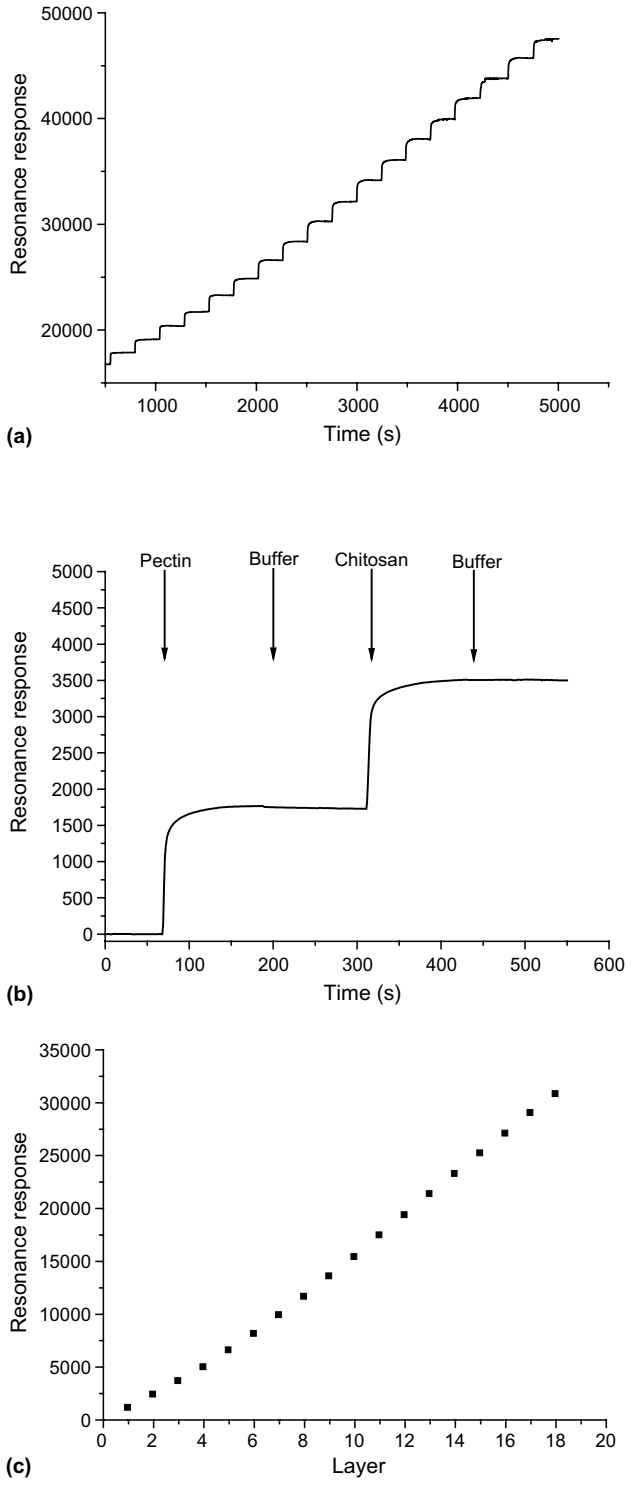

Figure 3. (a) Plot of resonance response versus time for the assembly of an 18-layer pectin/chitosan multilayer on a poly-L-Lysine base layer. (b) Detail of the resonance response versus time for the assembly of the seventh and eighth layers. (c) Resonance response as a function of layer number for a pectin/chitosan multilayer.

weight chitosan and pectin. The observed response consists of a series of step changes of approximately equal height. After biopolymer addition, the response quickly reaches a plateau. Fig. 3b shows a detail of the response for the seventh and eighth layers of pectin and low molecular weight chitosan, respectively, which shows the stability of the response during the buffer rinse. Under these conditions, the affinity of the biopolyelectrolytes for each other is high, and over these timescales, the binding of the biopolyelectrolyte to the charged surface is essentially irreversible. The surface plasmon response as a function of layer number is shown in Figure 3c. A smooth curve is obtained with little difference in response between successive pectin and chitosan layers. Initially, the response for each layer increases with increasing layer number, this is followed by a linear region and then some decrease in response at higher layer numbers. The total response, $\Delta\theta$, after 18 layers is $\sim$3.1°. For a uniform adsorbed layer, the sensor response is given by[39]

$$\Delta\theta = m(\eta_a - \eta_s)[1 - \exp(-2d/l_d)]$$

where η_a and η_s are the refractive indices of the adsorbed layer and solvent, respectively, m is the change in $\Delta\theta$ for a unit change in refractive index, d is the thickness of the film and l_d is a characteristic decay length of the evanescent electromagnetic field, and can be estimated as 37±13% of the wavelength of light at the surface plasmon resonance minimum.[39]

For the formation of multilayer polyelectrolyte films two growth regimes can be distinguished, linear and exponential,[7,16,15,40] Exponential growth was observed when there was diffusion of weakly associated polyelectrolyte within the film. Both the pectin and chitosan interactions are poorly reversible as indicated by the plateau in surface plasmon resonance response when the film is rinsed in buffer, indicating a relatively strong association. The multilayer may also grow linearly, although sometimes initial layers need to be deposited before linear growth is subsequently observed.[41] The surface plasmon resonance response for the successive adsorption of pectin and chitosan layers (Fig. 3c) is consistent with an essentially linear growth regime, although initial layers need to be deposited before linear growth is observed. The slight curvature in the plot of surface plasmon resonance response versus layer number for the latter layers is consistent with the film growing to a thickness, which is outside the regime, where the dependence of resonance response to a growing film of uniform refractive can no longer be approximated to linear. For a uniform film with a relationship between $\Delta\theta$ and d as shown in Eq. 1, this would be consistent with the multilayer having an average refractive index of $\sim$1.403 (40–50% w/w polysaccharide) with a total thickness, d, of 100 ± 20 nm. The value of d obtained for this number of layers is consistent with that obtained for other multilayers, which had a linear growth.[9]

4. Conclusions

In common with other oppositely charged biopolyelectrolytes, the alternating deposition of pectin and chitosan results in the formation of a multilayer structure. Multilayer formation was observed at a pH when both polymers carried a charge. Changing pH, resulting in suppression of charge on one of the polyelectrolytes, resulted in layer disassembly highlighting the importance of electrostatic interactions in multilayer formation and stability. Deposition was irreversible over practical timescales and the thickness of an individual layer showed a dependence on biopolymer concentration and was particularly marked for pectin.

Acknowledgements

The authors thank the BBSRC core strategic grant for financial support; the EC Commission for the award of a Marie Curie fellowship to M.M. (Contract Number QLK-1999-50512) and CP Kelco for providing the pectin sample.

References

1. Mattison, K. W.; Dubin, P. L.; Brittain, I. J. *J. Phys. Chem. B* **1998**, *102*, 3830–3836.
2. Zintchenko, A.; Rother, G.; Dautzenberg, H. *Langmuir* **2003**, *19*, 2507–2513.
3. Weinbreck, F.; de Vries, R.; Schrooyen, P.; de Kruif, C. G. *Biomacromolecules* **2003**, *4*, 293–303.
4. Decher, G. *Science* **1997**, *277*, 1232–1237.
5. Skepo, M.; Linse, P. *Macromolecules* **2003**, *36*, 508–519.
6. Mascotti, D. P.; Lohman, T. M. *Proc. Nat. Acad. Sci. U.S.A.* **1990**, *87*, 3142–3146.
7. Elbert, D. L.; Herbert, C. B.; Hubbell, J. A. *Langmuir* **1999**, *15*, 5355–5362.
8. Burke, S. E.; Barrett, C. J. *Biomacromolecules* **2003**, *4*, 1773–1783.
9. Richert, L.; Lavalle, P.; Payan, E.; Shu, X. Z.; Prestwich, G. D.; Stoltz, J. F.; Schaaf, P.; Voegel, J. C.; Picart, C. *Langmuir* **2004**, *20*, 448–458.
10. Shiratori, S. S.; Rubner, M. F. *Macromolecules* **2000**, *33*, 4213–4219.
11. Kato, N.; Schuetz, P.; Fery, A.; Caruso, F. *Macromolecules* **2002**, *35*, 9780–9787.
12. Kovacevic, D.; van der Burgh, S.; de Keizer, A.; Stuart, M. A. C. *Langmuir* **2002**, *18*, 5607–5612.
13. Dubas, S. T.; Schlenoff, J. B. *Macromolecules* **2001**, *34*, 3736–3740.
14. Schlenoff, J. B.; Dubas, S. T. *Macromolecules* **2001**, *34*, 592–598.
15. Hubsch, E.; Ball, V.; Senger, B.; Decher, G.; Voegel, J. C.; Schaaf, P. *Langmuir* **2004**, *20*, 1980–1985.
16. Lavalle, P.; Gergely, C.; Cuisinier, F. J. G.; Decher, G.; Schaaf, P.; Voegel, J. C.; Picart, C. *Macromolecules* **2002**, *35*, 4458–4465.
17. Richert, L.; Lavalle, P.; Vautier, D.; Senger, B.; Stoltz, J. F.; Schaaf, P.; Voegel, J. C.; Picart, C. *Biomacromolecules* **2002**, *3*, 1170–1178.
18. Schols, H. A.; Posthumus, M. A.; Voragen, A. G. J. *Carbohydr. Res.* **1990**, *206*, 117–129.
19. Schols, H. A.; Voragen, A. G. J. *Carbohydr. Res.* **1994**, *256*, 83–95.
20. Berth, G.; Dautzenberg, H.; Rother, G. *Carbohydr. Polym.* **1994**, *25*, 177–185.
21. Marudova, M.; MacDougall, A. J.; Ring, S. G. *Carbohydr. Res.* **2004**, *339*, 1933–1939.
22. Marudova, M.; MacDougall, A. J.; Ring, S. G. *Carbohydr. Res.* **2004**, *339*, 209–216.
23. Sorlier, P.; Rochas, C.; Morfin, I.; Viton, C.; Domard, A. *Biomacromolecules* **2003**, *4*, 1034–1040.
24. Colfen, H.; Berth, G.; Dautzenberg, H. *Carbohydr. Polym.* **2001**, *45*, 373–383.
25. Benitez, M. J.; Jimenez, J. S. *Anal. Biochem.* **2002**, *302*, 161–168.
26. Brown, W. *Dynamic Light Scattering*; Oxford Science Publications: Oxford, 1993.
27. Needs, P. W.; Rigby, N. M.; Ring, S. G.; MacDougall, A. J. *Carbohydr. Res.* **2001**, *333*, 47–58.
28. Sorlier, P.; Denuziere, A.; Viton, C.; Domard, A. *Biomacromolecules* **2001**, *2*, 765–772.
29. Kohn, R. *Carbohydr. Res.* **1975**, *42*, 371–397.
30. Berth, G.; Dautzenberg, H. *Carbohydr. Polym.* **2002**, *47*, 39–51.
31. Berth, G.; Dautzenberg, H.; Rother, G. *Carbohydr. Polym.* **1994**, *25*, 187–195.
32. Berth, G.; Dautzenberg, H.; Hartmann, J. *Carbohydr. Polym.* **1994**, *25*, 197–202.
33. Schatz, C.; Pichot, C.; Delair, T.; Viton, C.; Domard, A. *Langmuir* **2003**, *19*, 9896–9903.
34. Glaser, R. W. *Anal. Biochem.* **1993**, *213*, 152–161.
35. Lahiri, J.; Isaacs, L.; Grzybowski, B.; Carbeck, J. D.; Whitesides, G. M. *Langmuir* **1999**, *15*, 7186–7198.
36. Ramsden, J. J. *Quart. Rev. Biophys.* **1994**, *27*, 41–105.
37. vanEijk, M. C. P.; Stuart, M. A. C. *Langmuir* **1997**, *13*, 5447–5450.
38. Wertz, C. F.; Santore, M. M. *Langmuir* **2002**, *18*, 706–715.
39. Jung, L. S.; Campbell, C. T.; Chinowsky, T. M.; Mar, M. N.; Yee, S. S. *Langmuir* **1998**, *14*, 5636–5648.
40. Picart, C.; Lavalle, P.; Hubert, P.; Cuisinier, F. J. G.; Decher, G.; Schaaf, P.; Voegel, J. C. *Langmuir* **2001**, *17*, 7414–7424.
41. Caruso, F.; Niikura, K.; Furlong, D. N.; Okahata, Y. *Langmuir* **1997**, *13*, 3422–3426.